# Supporting Information for 'Homeostatic mechanisms regulate distinct aspects of cortical circuit dynamics'

Yue Kris Wu, Keith B. Hengen, Gina G. Turrigiano and Julijana Gjorgjieva

## Supplementary Figures

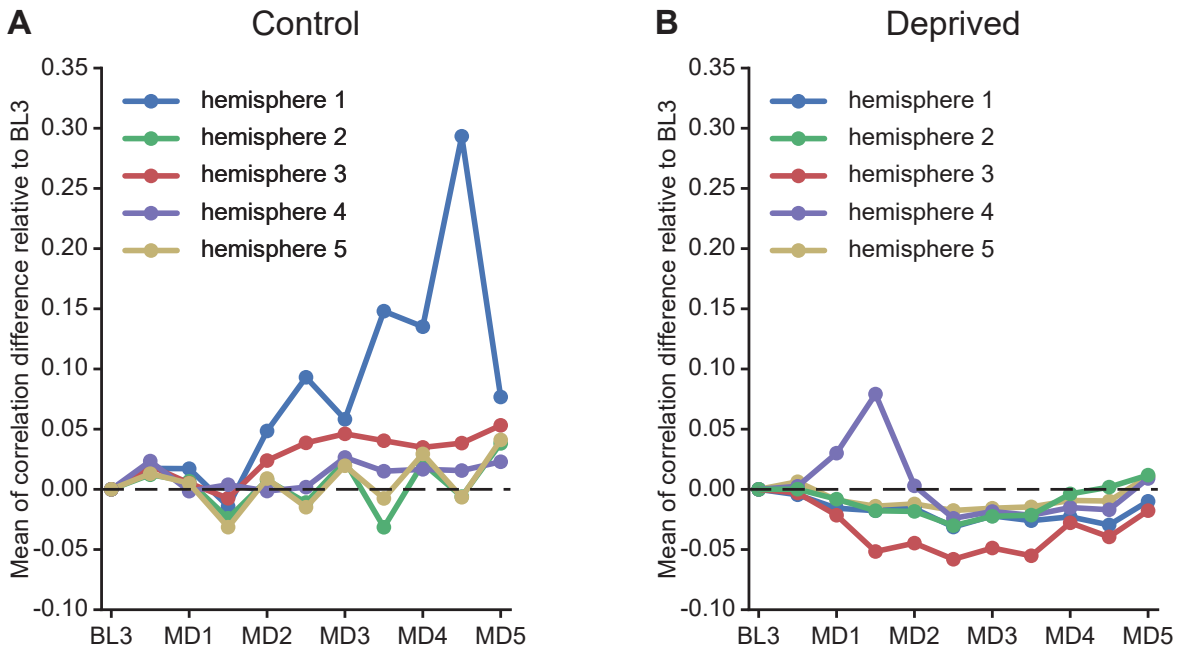


**Fig. S1.** Change in correlations of individual hemispheres. (A) Correlation differences relative to baseline of five control hemispheres. (B) Same as A but for five deprived hemispheres. Note that for deprived hemispheres 2 and 4, correlations at MD3 are used for the slope analysis (see Fig. 1E, right).



www.pnas.org/cgi/doi/10.1073/pnas.1918368117

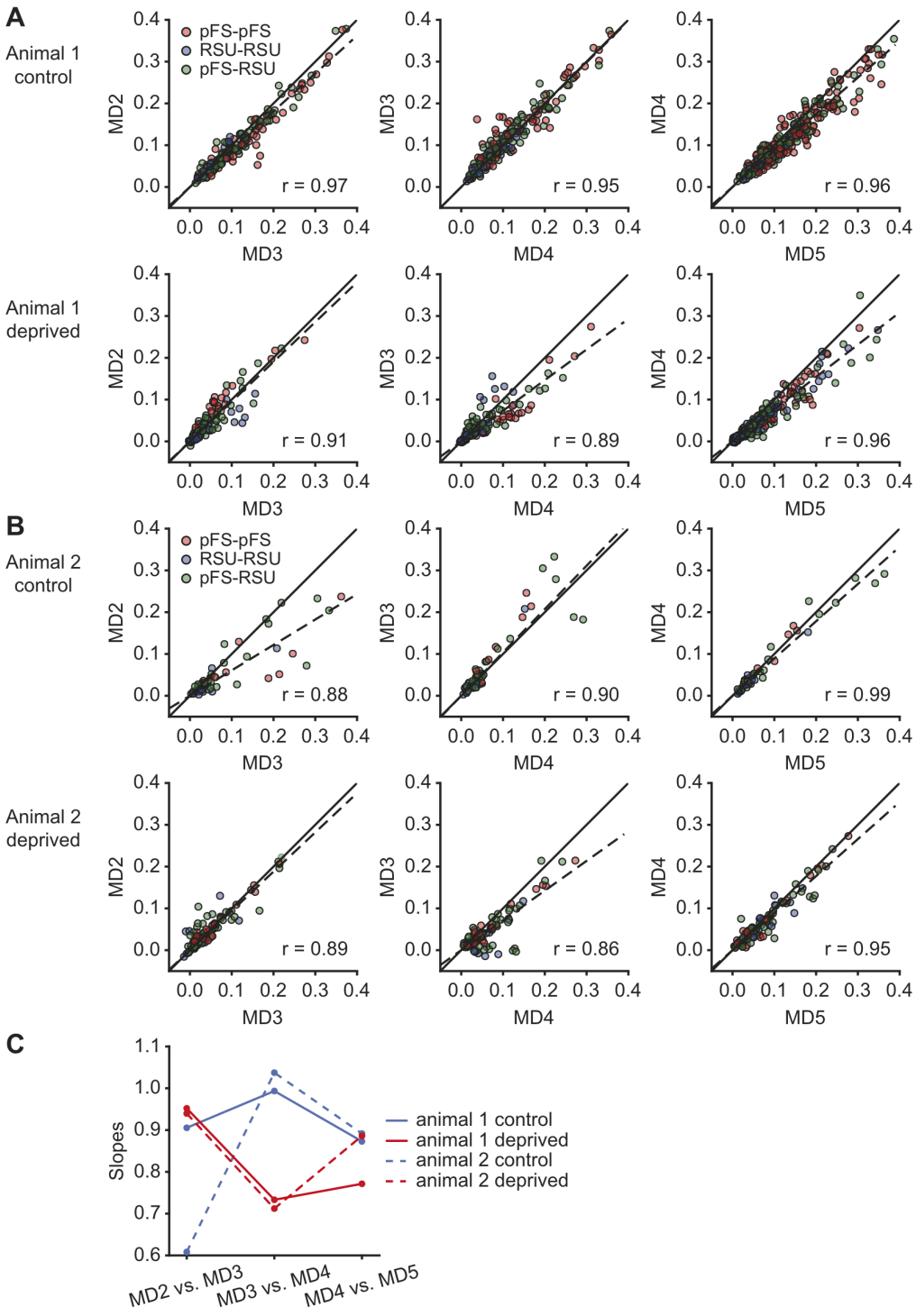


**Fig. S2.** (A) Top: correlation comparisons between MD2 and MD3 (left), between MD3 and MD4 (middle), and MD4 and MD5 (right) at the single cell-pair level of a control hemisphere from one animal. Different colors represent the correlations between different neuron types. Dashed lines are fitted regression lines crossing the origin. Bottom: same as top but for the deprived hemisphere from the same animal. (B) Same as A but for another animal. (C) Slopes of fitted regression lines for the correlation comparisons in A and B.

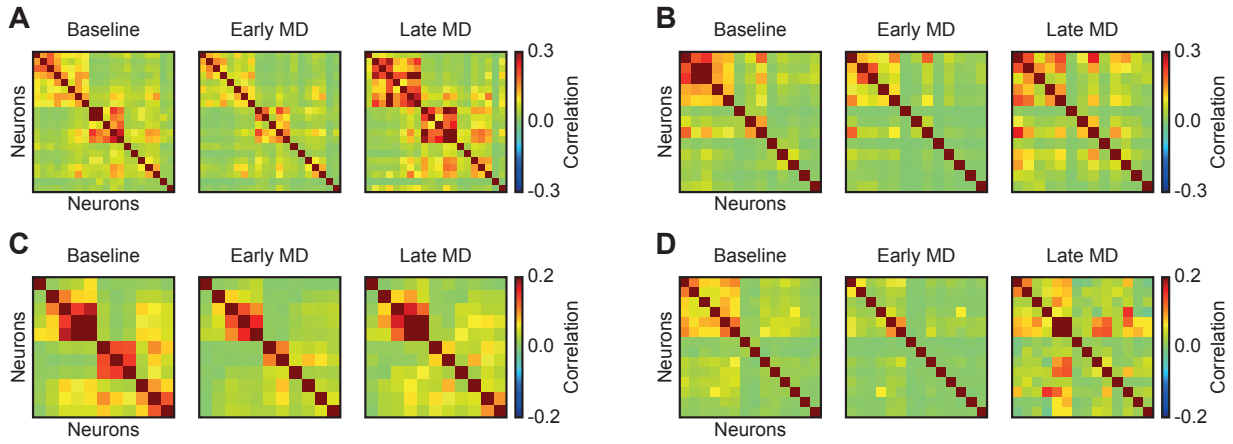


**Fig. S3.** Correlation matrices from other deprived hemispheres at three different time points. Each panel is a different deprived hemisphere.

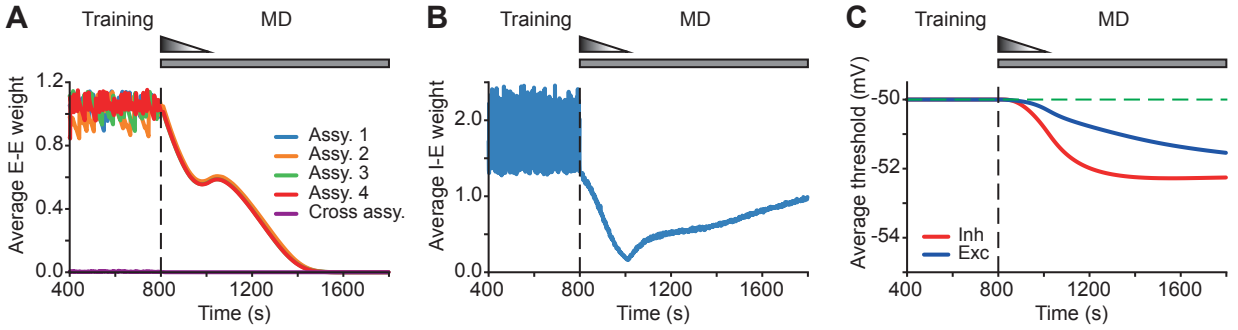


**Fig. S4.** Weights and neuronal thresholds in the model with persistent Hebbian LTD and homeostatic plasticity. (A) Average excitatory-to-excitatory weights for each assembly and across assemblies. The vertical dashed line indicates the onset of MD. (B) Average inhibitory-to-excitatory weights which target all excitatory neurons independent of assembly membership. (C) Average firing thresholds of excitatory (blue) and inhibitory (red) neurons. The horizontal dashed line indicates the initial firing threshold. The shaded gray triangle indicates the linear decrease of thalamocortical connections onto both excitatory and inhibitory neurons, while the gray rectangle indicates the continuous action of different homeostatic mechanisms, as in Figures 4.

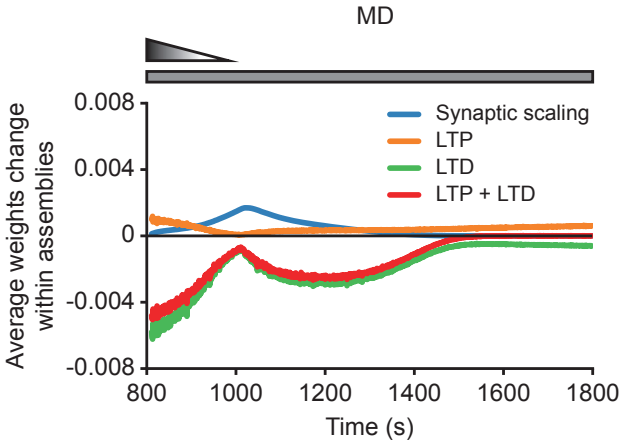


**Fig. S5.** Average weight change within assemblies induced by the different synaptic plasticity and homeostatic mechanisms. The shaded gray triangle indicates the linear decrease of thalamocortical connections onto both excitatory and inhibitory neurons, while the gray rectangle indicates the continuous action of different homeostatic mechanisms, as in Figure 4.

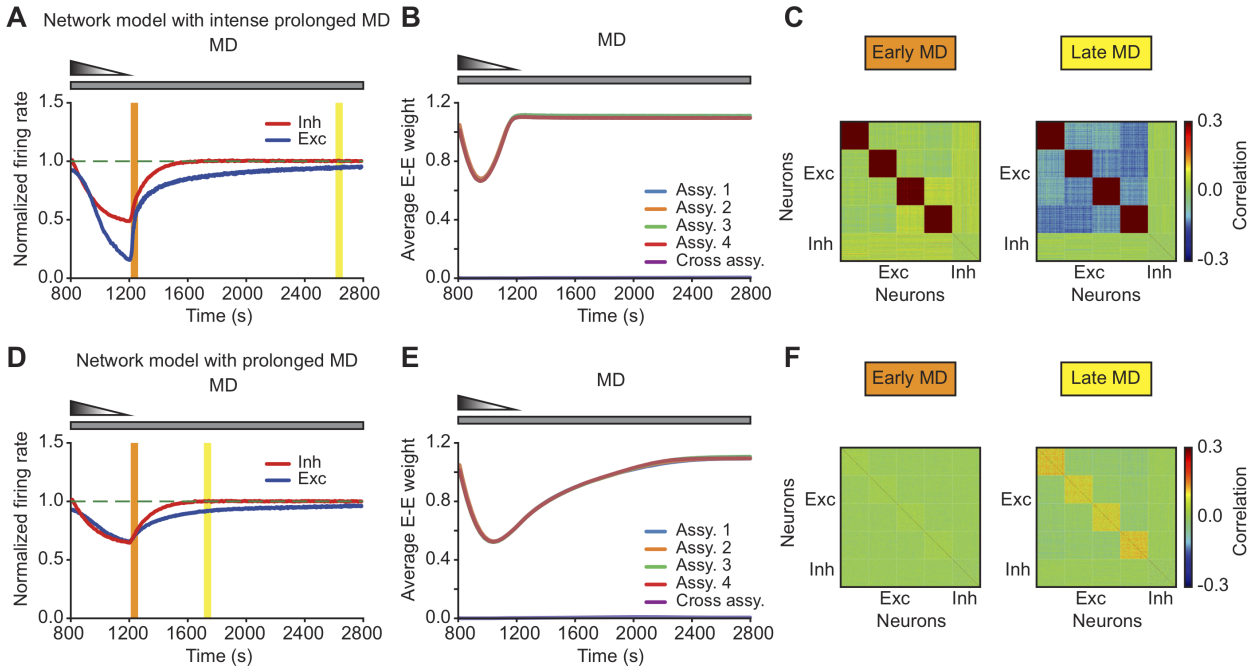


**Fig. S6.** Top (A-C): More intense and prolonged thalamocortical LTD during MD in the model. The feedforward thalamocortical connections onto excitatory and inhibitory neurons linearly decreased by 15% and 20% from 810 seconds to 1210 seconds. (A) The average normalized firing rates of excitatory (blue) and inhibitory (red) neurons. (B) Average excitatory-to-excitatory weights for each assembly and across assemblies. (C) Correlation matrix during the orange region in A (left) immediately after feedforward connections stop decreasing, and during the yellow region in A (right) where firing rates have recovered to 90% of their baseline. Bottom (D-F): Prolonged thalamocortical LTD during MD in the model. The feedforward thalamocortical connections onto excitatory and inhibitory neurons linearly decreased by 8% and 15% from 810 seconds to 1210 seconds. (D) Same as A. (E) Same as B. (F) Same as C. In A,B,D,E, the shaded gray triangle indicates the linear decrease of thalamocortical connections onto both excitatory and inhibitory neurons, while the gray rectangle indicates the continuous action of different homeostatic mechanisms, as in Figure 4.

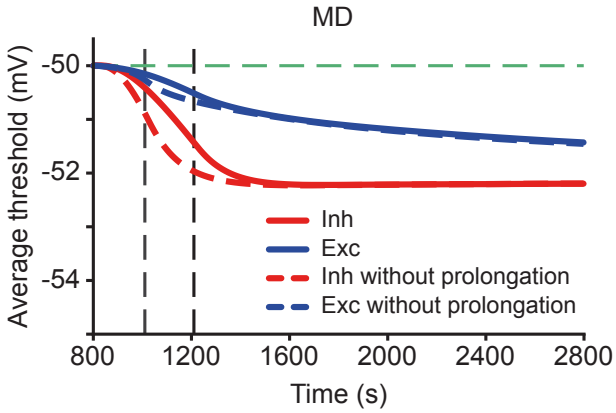


**Fig. S7.** Comparison of average firing thresholds of excitatory (blue) and inhibitory (red) neurons between the models with normal (as in the main manuscript) and prolonged (as in Fig. S6) thalamocortical LTD. The horizontal dashed line indicates the initial firing threshold. The first vertical dashed line indicates the offset of thalamocortical LTD for the model as in the main manuscript, while the second vertical dashed line indicates the prolonged offset for the model as in Fig. S6.

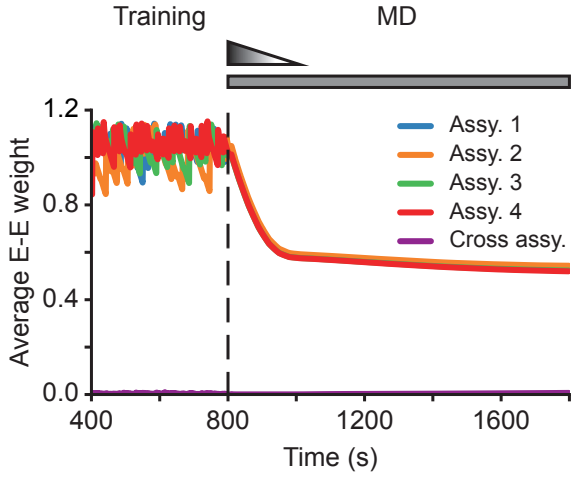


**Fig. S8.** Average excitatory-to-excitatory weights for each assembly and across assemblies without synaptic scaling. The vertical dashed line indicates the onset of MD. The shaded gray triangle indicates the linear decrease of thalamocortical connections onto both excitatory and inhibitory neurons, while the gray rectangle indicates the continuous action of different homeostatic mechanisms, as in Figure 4.

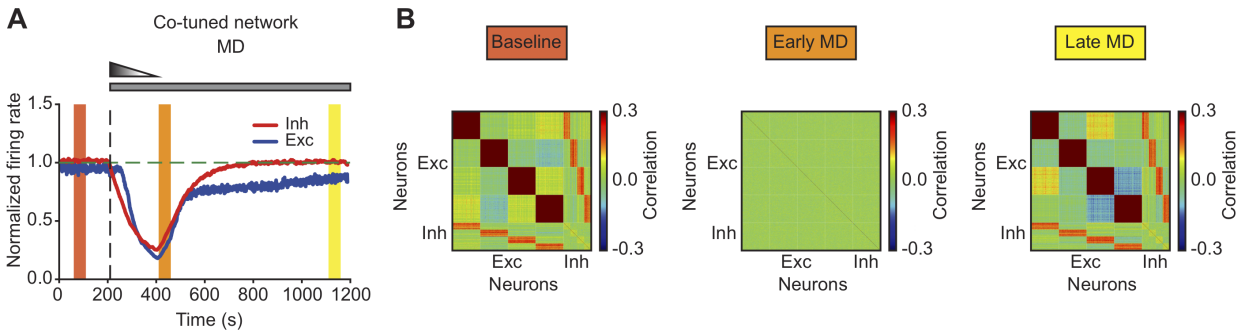


**Fig. S9.** Changes of firing rates and correlations during MD in the co-tuned networks. (A) The average normalized firing rates of excitatory (blue) and inhibitory (red) neurons. The vertical dashed line indicates the onset of MD. The horizontal dashed line indicates a normalized firing rate of 1.0. The shaded gray triangle indicates the linear decrease of thalamocortical connections onto both excitatory and inhibitory neurons, while the gray rectangle indicates the continuous action of different homeostatic mechanisms, as in Figure 4. (B) Correlation matrix at baseline (left, brown region in A), at early MD (middle, orange region in A) and at late MD (right, yellow region in A).

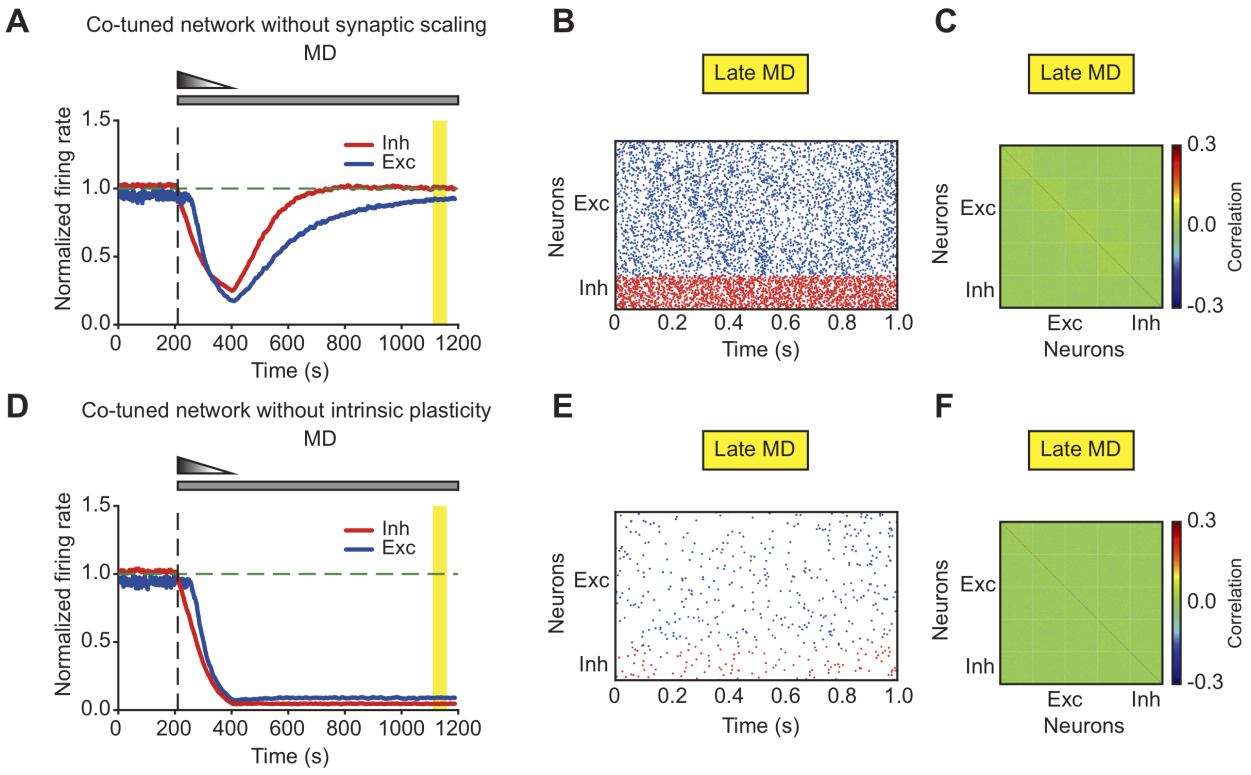


**Fig. S10.** Individual homeostatic mechanisms have different functionality during MD in the co-tuned networks. (A, D) The average normalized firing rates of excitatory (blue) and inhibitory (red) neurons without synaptic scaling (A) or without intrinsic plasticity (D). The vertical dashed line indicates the onset of MD. The horizontal dashed line indicates a normalized firing rate of 1.0. (B, E) Spontaneous activity of excitatory (blue) and inhibitory (red) neurons during late MD without synaptic scaling (B) or without intrinsic plasticity (E). (C, F) Correlation matrix during late MD indicated by the yellow region in A, D, without synaptic scaling (C) or without intrinsic plasticity (F). In A,D, the shaded gray triangle indicates the linear decrease of thalamocortical connections onto both excitatory and inhibitory neurons, while the gray rectangle indicates the continuous action of different homeostatic mechanisms, as in Figure 4.

## Supplementary Table

**Table S1: Co-tuned Network Model Parameters**

| Symbol | Value | Unit | Description |
|---|---|---|---|
| $J^{II}$ | 0.1 | - | I-to-I connection weight |
| $J^{\text{ext}\to E}$ | 0.75 | - | Initial external-to-E connection weight |
| $J^{\text{ext}\to I}$ | 0.76 | - | Initial external-to-I connection weight |
| $A^{-}$ | 0.0091 | - | Amplitude of LTD |
| $\tau^{\text{ss}}$ | 300 | s | Time constant of synaptic scaling |
| $\eta^{\text{ip}}$ | 0.0005 | mV/s | Learning rate of intrinsic plasticity |

## Supplementary Text

Here we demonstrate that synaptic scaling alone in the absence of intrinsic plasticity cannot recover the inhibitory firing rates when excitatory and inhibitory connections onto inhibitory neurons (E-to-I and I-to-I connection) do not change during MD. We also demonstrate that the addition of intrinsic plasticity enables the recovery of inhibitory firing rates.

The firing rate of inhibitory neurons at baseline can be described by the following equation (1, 2):

$$\tau_I \frac{dr_I^{\mathsf{BL}}}{dt} = -r_I^{\mathsf{BL}} + f(J_{IE} r_E^{\mathsf{BL}} - J_{II} r_I^{\mathsf{BL}} + g_I) \tag{1}$$

where $r_E^{\mathsf{BL}}$ and $r_I^{\mathsf{BL}}$ are the average firing rate of excitatory neurons and inhibitory neurons at baseline, respectively, $\tau_I$ is the time constant of inhibitory firing dynamics, $J_{IE}$ and $J_{II}$ denote the average synaptic strength from excitatory and inhibitory neurons onto inhibitory neurons, $g_I$ is the feedforward input onto inhibitory neurons at baseline and $f$ is the input-output function of the inhibitory population.

Similarly, the firing rate of inhibitory neurons at MD can be expressed as follows:

$$\tau_I \frac{dr_I^{\mathsf{MD}}}{dt} = -r_I^{\mathsf{MD}} + f(J_{IE} r_E^{\mathsf{MD}} - J_{II} r_I^{\mathsf{MD}} + g_I - \Delta g_I) \tag{2}$$

where $\Delta g_I$ is the amount of change in the feedforward input onto inhibitory neurons since feedforward drive is reduced following MD.

To simplify the analysis, we assume that the input-output function is a linear function. Here we assume a gain of $\alpha$, but we note that the gain of the input-output function can be controlled by intrinsic plasticity because it denotes how excitable the population firing rate is as a function of total synaptic input:

$$\tau_I \frac{dr_I^{\mathsf{BL}}}{dt} = -r_I^{\mathsf{BL}} + \alpha \left( J_{IE} r_E^{\mathsf{BL}} - J_{II} r_I^{\mathsf{BL}} + g_I \right) \tag{3}$$

$$\tau_I \frac{dr_I^{\mathsf{MD}}}{dt} = -r_I^{\mathsf{MD}} + \alpha \left( J_{IE} r_E^{\mathsf{MD}} - J_{II} r_I^{\mathsf{MD}} + g_I - \Delta g_I \right). \tag{4}$$

If we assume that $J_{IE}$ and $J_{II}$ do not change during MD, and there is no intrinsic plasticity at baseline and during MD which changes the input-output gain, then we can calculate the steady states of inhibitory firing rates in these two different time periods in terms of the firing rates of excitatory neurons

$$r_I^{\mathsf{BL}} = \alpha(J_{IE} r_E^{\mathsf{BL}} + g_I)/(1 + \alpha J_{II}) \tag{5}$$

$$r_I^{\mathsf{MD}} = \alpha(J_{IE} r_E^{\mathsf{MD}} + g_I - \Delta g_I)/(1 + \alpha J_{II}). \tag{6}$$

Therefore, given our assumption that $J_{IE}$ and $J_{II}$ do not change during MD, and the result from the data that excitatory firing rates recover to the baseline during prolonged MD, leads us to conclude that the inhibitory firing rates during MD are always smaller than at baseline

$$r_I^{\mathsf{MD}} < r_I^{\mathsf{BL}} \tag{7}$$

Without intrinsic plasticity, inhibitory firing rates therefore cannot recover under the above assumptions. If, however, we allowed for intrinsic plasticity to change the gain of the inhibitory population to $\beta$, then Eq. 4 becomes

$$\tau_I \frac{dr_I^{\mathsf{MD}}}{dt} = -r_I^{\mathsf{MD}} + \beta \left( J_{IE} r_E^{\mathsf{MD}} - J_{II} r_I^{\mathsf{MD}} + g_I - \Delta g_I \right). \tag{8}$$

At steady state,

$$r_I^{\mathsf{MD}} = \beta(J_{IE} r_E^{\mathsf{MD}} + g_I - \Delta g_I)/(1 + \beta J_{II}) \tag{9}$$

so that the condition that the firing rates at MD recover to that at baseline leads to

$$\alpha(J_{IE} r_E^{\mathsf{BL}} + g_I)/(1 + \alpha J_{II}) = \beta(J_{IE} r_E^{\mathsf{MD}} + g_I - \Delta g_I)/(1 + \beta J_{II}). \tag{10}$$

This implies that there exists a solution for intrinsic plasticity to modify the gain $\beta$ of the inhibitory population, so that the inhibitory firing rates at MD recover to that at baseline. We note that the results would also hold for nonlinear input-output functions $f$ assuming that they are monotonically increasing as a function of synaptic input, which is the case for many commonly used functions like a threshold-linear or sigmoidal nonlinearities.

We further analyze under which conditions inhibitory firing rates can recover by changing either E-to-I connections or I-to-I connections in the absence of intrinsic plasticity.
If we allow excitatory connections onto inhibitory neurons $J_{IE}$ to be plastic while keeping inhibitory connections onto inhibitory neurons $J_{II}$ static, the firing rate of inhibitory neurons at baseline and MD can be described as follows,

$$\tau_I \frac{dr_I^{\mathsf{BL}}}{dt} = -r_I^{\mathsf{BL}} + \alpha \left( J_{IE}^{\mathsf{BL}} r_E^{\mathsf{BL}} - J_{II} r_I^{\mathsf{BL}} + g_I \right) \tag{11}$$

$$\tau_I \frac{dr_I^{\mathsf{MD}}}{dt} = -r_I^{\mathsf{MD}} + \alpha \left( J_{IE}^{\mathsf{MD}} r_E^{\mathsf{MD}} - J_{II} r_I^{\mathsf{MD}} + g_I - \Delta g_I \right). \tag{12}$$

We then obtain the condition that firing rates of inhibitory neurons at MD recover to that at baseline

$$J_{IE}^{\mathsf{MD}} = J_{IE}^{\mathsf{BL}} + \frac{\Delta g_I}{r_E^{\mathsf{BL}}} \tag{13}$$

If inhibitory connections onto inhibitory neurons $J_{II}$ are plastic while excitatory connections onto inhibitory neurons $J_{IE}$ static, the firing rate of inhibitory neurons at baseline and MD can be expressed by

$$\tau_I \frac{dr_I^{\mathsf{BL}}}{dt} = -r_I^{\mathsf{BL}} + \alpha \left( J_{IE} r_E^{\mathsf{BL}} - J_{II}^{\mathsf{BL}} r_I^{\mathsf{BL}} + g_I \right) \tag{14}$$

$$\tau_I \frac{dr_I^{\mathsf{MD}}}{dt} = -r_I^{\mathsf{MD}} + \alpha \left( J_{IE} r_E^{\mathsf{MD}} - J_{II}^{\mathsf{MD}} r_I^{\mathsf{MD}} + g_I - \Delta g_I \right). \tag{15}$$

The condition that firing rates of inhibitory neurons at MD recover to that at baseline is

$$J_{II}^{\mathsf{MD}} = J_{II}^{\mathsf{BL}} - \frac{\Delta g_I}{r_I^{\mathsf{BL}}} \tag{16}$$

Therefore, the analysis indicates that the firing rates of inhibitory neurons can recover if either E-to-I or I-to-I connections is plastic and either the above-listed condition is fulfilled.

## References


1. Dayan, P. and Abbott, L. F. (2001). *Theoretical neuroscience: Computational and mathematical modeling of neural systems*. The MIT Press. Cambridge, Massachusetts.

2. Tsodyks, M. V., Skaggs, W. E., Sejnowski, T. J., and McNaughton, B. L. (1997). Paradoxical effects of external modulation of inhibitory interneurons. *Journal of Neuroscience*, 17(11):4382–4388.